

Atenolol degradation using hybrid processes of ultraviolet/peroxymonosulfate/microwave: modeling and optimization with artificial neural network and PSO algorithm

Maryam Razaghi^{a,b}, Bahare Dehdashti^{a,b,c,*}, Farzaneh Mohammadi^a, Zeynab Moradmand^{a,b}, Nasrin Zahedi^{a,b}, Mohammad Mehdi Amin^{a,c,*}

^aDepartment of Environmental Health Engineering, School of Health, Isfahan University of Medical Sciences, Isfahan, Iran, Tel.: +989132162677; email: baharehdehdashty@gmail.com (B. Dehdashti), Tel.: +989133670508; email: mohammadmehdia@gmail.com (M.M. Amin)

^bStudent Research Committee, School of Health, Isfahan University of Medical Sciences, Isfahan, Iran

^cEnvironment Research Center, Research Institute for Primordial Prevention of Non-communicable Disease, Isfahan University of Medical Sciences, Isfahan, Iran

Received 24 March 2023; Accepted 28 July 2023

ABSTRACT

Atenolol (ATN) belongs to a class of drugs known as β -blockers. This medicine works on the heart and blood vessels by blocking the action of some natural chemicals in the body. ATNs are present in surface water and sediments from hospitals and wastewater treatment plants. In the current study ATN degradation using hybrid processes of peroxymonosulfate (PMS)/ultraviolet (UV)/microwave (MW) were investigated. The reaction kinetics and scavengers' effects were also evaluated. Experiments were carried out in a 1.5-L reactor with UV lamp and MW and then analyzed by high-performance liquid chromatography. Artificial neural networks was implemented for modelling and particle swarm optimization technique was used to specify the optimal status for ATN degradation. According to the result, only MW power and PMS parameters had a linear relationship with efficiency, and other parameters had non-linear relationship. Moreover, increasing PMS dosage and MW power in neutral pH has a significant effect on ATN degradation. As per our result, optimum conditions in the experiments were pH 6.2 and 28.8 mg/L ATN initial concentration, 3.05 mg/L PMS concentration, 14.30 min UV time, 19.90 min MW time and 630 W MW power. In this situation the ATN degradation rate was about 97% which according to the sensitivity analysis by Pearson correlation method, pH had the greatest effect on the degradation efficiency in the range of 3–7. Nitrate (NO_3^-), chloride (Cl^-) and humic acid (HA) were used as scavengers. The findings showed that increasing the concentration in HA and NO_3^- decreased the efficiency, but Cl^- did not have much effect on the results. According to the results, this method can be efficient for the degradation of ATN.

Keywords: Advanced oxidation; Artificial neural networks modeling; Atenolol; Hybrid processes; Particle swarm optimization

1. Introduction

Personal care products (PPCPs) and pharmaceuticals are emerging pollutants that prompt great attention in

recent decades. Atenolol (ATN) is one of the most common β -blocker belongs to PPCPs [1,2]. β -blockers are widely used to treat high blood pressure, arrhythmia and other cardiovascular diseases [3,4]. Due to the widespread use

* Corresponding authors.

of β -blockers, they usually remain in the aquatic environment [3]. On the other hand, pharmaceutical wastewaters have high dissolved solids as well as dissolved organic carbon. Discharge of the wastewaters to the environment have rigid difficulties such as formation of antibiotic resistant microbes in the aqueous environment and increased the chemical toxicity [4]. ATN was generally discovered in wastewater and surface waters, with a concentration range of ng/L to $\mu\text{g/L}$ [5]. The bioaccumulation, biological activity, persistence and toxicity of ATN make it a major threat to the ecosystem. Its presence along with other β -blockers can create synergistic toxicity in the environment. Prolonged exposure to ATN causes hormonal imbalance and cancer in humans. It has also been reported that ATN can have a negative effect on the growth of human embryonic cells in combination with other common therapeutic drugs. For these reasons, it is necessary to remove atenolol from wastewater with effective treatment processes [6,7]. Recently, some of the methods have been used for ATN degradation including modified multiwalled carbon nanotubes [8], photocatalytic reactor with immobilized ZnO [9], and ZnO/solar irradiation [10]. The advanced oxidation processes (AOPs) alone or in combination with other treatment methods are useful options to remove organic pollutants from wastewater [11]. AOPs are extremely efficient wastewater treatment technologies for degradation of recalcitrant organic material [12], low biodegradability, resisting, disincentive, wide chemical stability contaminants [13] and pharmaceuticals [14]. AOPs are the oxidation processes associated to the generation of reactive oxygen species (ROS) such as hydroxyl radicals ($\text{OH}\cdot$), sulfate radicals ($\text{SO}_4^{\cdot-}$), and single oxygen by activation of oxidants, which stimulate the velocity of reaction. [11,15]. Also, another advantage of the AOPs is that working at ambient temperature [13].

Peroxymonosulfate ($\text{PMS}:\text{HSO}_5^-$) is a convenient chemical oxidant for removing several organics. PMS is an ecological friendly oxidant that used in environmental remediation applications. Also, it has many uses due to its reasonable cost, very wide stability, solubility and function in large range of pH [15,16]. PMS is generally activated by using ultraviolet light, carbon catalysts, heat, ultrasound [17], heterogeneous catalytic materials and microwave [18]. In some studies, the researchers used sulfate radical for removing different pollutants, for example, Mohamadiyan et al. [19] used it for aniline degradation from aqueous solution.

Ultraviolet (UV) radiation is a method with many advantages such as high effectiveness to pathogens, easy proceeds, chemical-free and no by-product formation. The research and usage of UV has been rapidly growing especially [20] in sterilization of medical devices, water and air treatment systems [21]. Recently, UV has been used in many studies to remove various pollutants such as azo red-60 dye from textile effluents, bisphenol A from treated wastewaters, and etc [22,23].

Nowadays, microwave (MW) irradiation technology has attracted an increasing attention as a powerful tool in several energy and environmental applications [24,25]. MW heating is a procedure of effective quick heating material in relatively enclosed volumes via the sorption and scattering of MW energy [26,27]. Compared to normal heating techniques, MW heating is rapid, more effective and flexible, it

doesn't need direct closeness among the heating origin and the objects, very cost-effective and heating materials homogeneously [24,26]. One essential step in the AOPs is to model and optimization of effective parameters in the process. One of the traditional methods of modeling is regression. Artificial neural networks are preferable to regression models. Neural networks offer a number of advantages, including requiring less formal statistical training, ability to implicitly detect complex non-linear relationships between dependent and independent variables, ability to detect all possible interactions between predictor variables, and the availability of multiple training algorithms [28]. Currently, one of the best forecasting and optimization strategies is the use of artificial intelligent models in addition to evolutionary algorithms, like artificial neural networks (ANNs) and particle swarm optimization (PSO) technique, which have been applied in many studies [29].

ANN is an information processing model containing by many interconnected neurons that was generally inspired of the human brain [30]. Recently, ANNs are becoming a popular further owing to their decreased computation time, great precision, and capability to non-linearly map relationships among the inputs and outputs of a system. The usage of ANNs is not only limited to function estimation but also involve classification, prediction, pattern recognition, and image processing [31]. PSO technique is a relatively recent empirical search method whose mechanics are stimulated by the crowding or cooperation behavior of biological populations. The PSO algorithm could be applied to dissolve barriers that are not truly suited for standard optimization algorithms, including problems in which the objective function is discontinuous, accidental, or extremely non-linear [29]. Therefore, the aim of this study was to investigate the efficiency of the integrated process of ultraviolet, peroxy-monosulfate and microwave for degradation of ATN from aqueous solutions by using the response surface method. Moreover, for prediction and optimization of experimental data ANN and PSO algorithm were used, respectively. Also, in order to investigate the trend of changes in the concentration of ATN over time, the kinetics of the reaction was investigated.

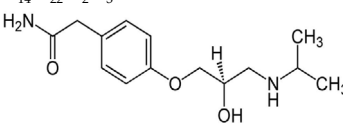
2. Materials and methods

2.1. Materials and reagents

Atenolol chemical name known as 2-[4-[2-hydroxy-3-(propan-2-ylamino)propoxy]phenyl]acetamide [32], with reported purities of >98%, was obtained from Raha Pharmaceutical Factory (Isfahan, Iran). Its properties are reported in Table 1. Potassium peroxymonosulfate (KHSO_5), potassium dihydrogen phosphate (PDP) and humic acid (HA) were purchased from Merck. High-performance liquid chromatography (HPLC)-grade acetonitrile and methanol (for rinsing injection needle) also were purchased from Merck (Germany).

ATN stock solution was prepared by adding 1 g of ATN powder to 1 L of deionized water and well mixed with a magnetic stirrer. HA stock solution was prepared by adding 0.3 g of dry HA powder to 1 L of deionized water, and stirring overnight. The pH of solutions was adjusted with

Table 1
Properties of atenolol

Properties	Amount
Chemical formula	C ₁₄ H ₂₂ N ₂ O ₃
Chemical structure	
Solubility (mg/mL)	13.3
Molecular weight (g/mol)	266.34
pKa	9.6
logK _{ow}	0.16

0.1 M HCl for pH < 6 and buffered with 0.1 M NaOH for 6 < pH < 12.

2.2. Experimental procedures

The experiments were accomplished in a sealed 1.5 L, two-chamber reactor containing 0.5 L of sample in the inner chamber. In the outer chamber, water was placed to keep the sample cool. Three low-pressure mercury UV lamp (Osram, G6T5/OF, 6W, ozone-free) was set in the middle of the reactor. ATN and PMS were mixed with determined concentrations and pH was adjusted for each sample. Then the sample was injected into the pilot. Due to the UV lamp, the pilot was completely enclosed by aluminum foil. Immediately after the initial contact time, the sample was transferred to a round bottom flask and placed in the microwave. Graham's condenser was also connected to the flask from the center of the microwave. All of the tests were accomplished in an air-conditioned room about 23°C ± 2°C.

2.3. Analytical methods

The samples were analyzed by HPLC (Jasco Pu-2080, Japan) provided with a UV-Vis detector and a C18-Waters-spbcri-sorb column. The analysis was performed with a 30/70 (v/v) PDP as a buffer and acetonitrile as a mobile phase that set in pH 3.5 and the flow rate was set at 1.0 mL/min. The injection volume was 50 µL. The UV-Vis detector (Jasco UV-2075, Japan) was set in 231 nm.

2.4. Experimental design

In this study, central composite design (CCD) was used to design the experiments. Some proposed levels were slightly modified through user-defined mode to make them feasible in the laboratory. Experimental design was performed in Design-Expert 11.0 software. In this method, 5 levels were considered for each variable. Table 2 shows the considered variables and levels.

2.4.1. ANN modeling

The ANN was used to determine non-linear relations between variables. For the ANN modeling, MATLAB

Table 2
Variables and that levels in this study

Name	Minimum	Maximum	Levels
pH	3	11	3, 5, 7, 9, 11
Atenolol, mg/L	1	60	1, 10, 30, 50, 60
Time (UV), min	5	30	5, 10, 15, 20, 30
Power, W	150	850	150, 300, 450, 600, 850
Peroxymono-sulfate, mg/L	0.20	3.20	0.2, 0.4, 0.8, 1.6, 3.2
Time (MW), min	5	30	5, 10, 15, 20, 30

software R2017a version was applied with the neural network toolbox (nntool). A three-substrate feed onward back propagation neural network was developed by exerting the tangent sigmoid (tansig) and linear (purelin) transfer functions in hidden and output layers, respectively, with the traditional Levenberg Marquardt training algorithm. The ANN model was comprised of six input parameters including initial concentration, pH, PMS, UV time, MW time and power. The input data were scaled within the range of -1 to 1. The output layer consists of a neuron that shows the degradation efficiency. The 54 samples were randomly divided into three groups: training (70%), validation (15%) and experimental (15%). The equations presented by Mohammadi et al. [33] were applied to determine the number of neurons in the hidden layer. The precision of the optimized ANN model was specified by computing the specification factor (R^2) as well as the mean square errors (MSE) as reported by equations presented in the other studies.

2.4.2. PSO optimization

In particle swarm optimization, simple factors, called particles, move in the search area of an optimization issue. The situation of a particle shows a possible answer to the optimization obstacle. Every particle search toward higher situation in the search area via modifying its speed in accordance with laws basically inspired by behavioral pattern of birds group. PSO belongs to the class of congestion intellect techniques that are used to dissolve optimization issues. In this study, the PSO algorithm was implemented in MATLAB software R2017a version. PSO was used to specify the optimal conditions for ATN degradation using ANN model developed in this study as objective function. Fig. 1 shows the algorithm pseudo code of PSO generally [34].

In the PSO algorithm, the number of ingredients, inertia weight (ω) and cognition in addition to social learning factors (C_1 and C_2) were improved by testing and mistake. The outcomes are described below:

- The number of particles are between 10 and 100 with the optimal number of 20.
- C_1 between 1 and 2 with the optimum value of 1.5.
- C_2 between 1 and 2 with the optimum value of 1.5.
- ω between 0 and 1 with the optimum value of 0.4.
- Maximum number of repetitions: 100 [32].

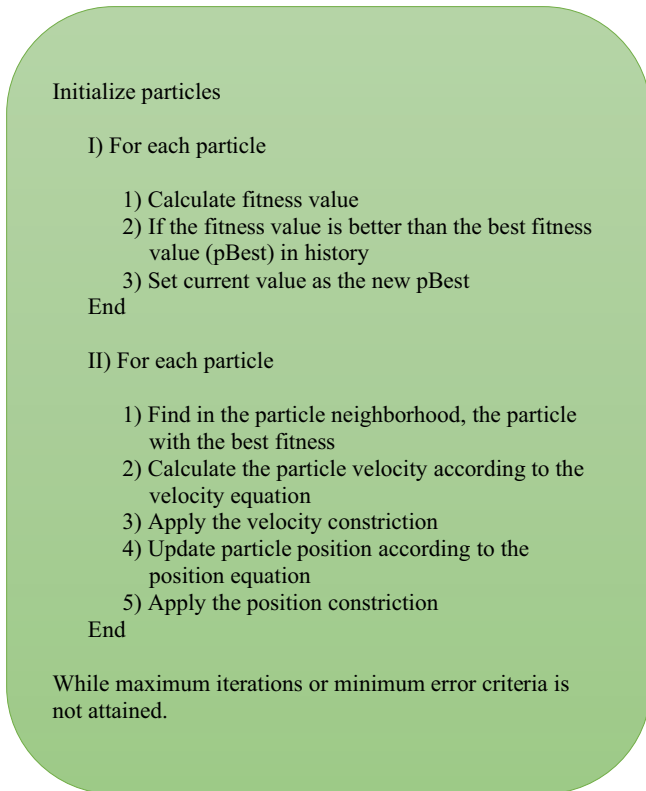


Fig. 1. Particle swarm optimization algorithm pseudo code.

3. Result and discussion

3.1. Modeling with ANN

Based on the intersection of mentioned equations in materials and methods section, a range of the number of hidden neurons is obtained, which in this research is equal to 4–8 neurons in hidden layer. To determine the best neural network topology, several networks with different numbers of hidden neurons [4–8] were developed and finally the 6:6:1 topology showed the best performance.

Fig. 2A shows the structure of a triple layer neural network that has 6 parameters in the input layer, 6 neurons in the hidden layer, and one parameter in the output layer.

Fig. 2B represents the training, validation and experiment errors against number of repetitions for the ANN models. In general, the error decreases after some epochs of training and the training algorithm terminates if the validation error enhance after six subsequence repetitions, or the restrictions of utmost error/epoch are trespassed. As demonstrated in the Fig. 2B the training algorithms for ANN are terminated in 5 epochs (because of validation error), whereas the training errors are tiny. The trial and validation error plots display resembling specifications; this is a symptom of properly apportioned data in this study. The MSE values of the validation step was equal to 2.625×10^{-4} .

The regression plots in Fig. 2C displays the network outputs with attention to purposes for training, validation, and experiment sets. For a thorough fit, the data should fall along a 45° line, where the network outputs are identical to

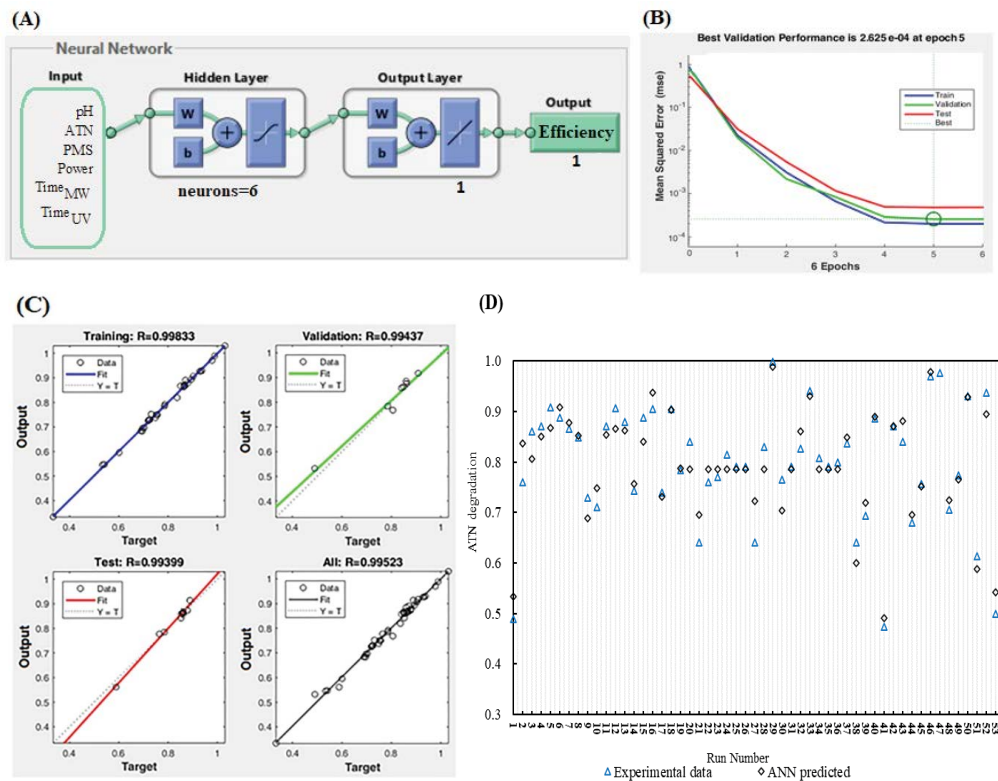


Fig. 2. (A) Developed artificial neural network structure, (B) performance, (C) regression plots, and (D) comparison of experimental and predicted results.

the purposes. It is apperceived that the output tracks the targets very good for training (0.998), validation (0.994), and experiment (0.993). Also, the coefficient of determination for the whole data was obtained 0.995. In this study, the network response is satisfying, and imagery could be used for entering new inputs. It is clear from the ANN results that no overfitting has occurred in developed network [35]. In Fig. 2D, a comparison diagram of the experimental and predicted results for 54 runs is presented.

3.2. Optimization with PSO

The PSO algorithm was used to optimize the input parameters to achieve the highest degradation efficiency. The designed neural network model was introduced as an objective function to PSO. Fig. 3B represents the optimum values of input parameters in the best iteration. Therefore, the optimal value of the input parameters, which are ATN, pH, PMS, UV time, MW time and power, were equal to 28.80 mg/L, 6.20 mg/L, 3.05 mg/L, 14.30 min, 19.90 min and 630 W, respectively, which leads to the highest degradation efficiency of 99.99%.

3.3. AOP performance in ATN degradation using ANN 3-dimensional graphs

Fig. 4A shows the interaction between ATN concentration and pH parameters on the ATN degradation rate within the changes in pH 3 to 11. It is clear that the initial concentration of ATN has non-linear relationship with the degradation efficiency, and by increasing it, the efficiency was improved initially, and after reaching the optimal efficiency, the degradation efficiency was reduced. In different pH values, the effect of the initial concentration on the degradation efficiency was the same. While in Yu et al. [5] study the ATN degradation slowly reduce with the increase of primary concentrations. On the other hand, the results of Vibhu research show an increase in degradation by increasing the concentration of ATN [36]. Generally, pH

plays a significant role in AOPs as it affects the specification of organics and the production of basic radical species [37]. pH has a non-linear relationship with the degradation efficiency, and increasing it to about 7 increases the degradation efficiency, but then decreases with increasing pH. These conditions have been observed in all concentrations examined. It's obvious that, in different initial concentration, the effect of the pH values on the degradation efficiency was the same. According to Hapeshi et al. [38], the pKa of ATN is 9.6, that at $6 < \text{pH} < 9.6$, the amino group could be protonated, while PMS ions are dominant in acidic conditions [39]. Therefore, the electrostatic attraction is increased and then the removal efficiency is increased. The results are consistent with the work of Liu et al. [40], wherein the most advantageous achievement has been detected in the pH range of 3–7 and also declined from 7.0 to 9.0. In addition, in the study of Gayathri et al. [41], RhB dye degradation increases slowly in pH 3 to 5 and strongly increases up to pH 7.

Fig. 4B shows the interaction between ATN concentration and PMS on the ATN degradation rate. PMS has a linear relationship with the ATN degradation at all initial concentrations. This means that increasing PMS increases degradation efficiency, regardless of the initial concentration. Liu et al. [40] found that there may be two reasons for this correlation. First, $\text{SO}_4^{\cdot-}$ reacted fast with ATN (the reported value is $k_{\text{SO}_4^{\cdot-}\text{-ATN}} = 2.2 \times 10^{10} \text{ L}/(\text{mol}\cdot\text{s})$). Second, $\text{SO}_4^{\cdot-}$ has a long half-life which generally because of its preference for electron transfer reaction [40]. The results are similar to those reported by Miao et al. [42]. This situation was different from that reported by Wu et al. [37], who found the K_{obs} visibly increased when the PMS concentration changed from 0 to 0.1 mM and further increase in PMS reduce the K_{obs} [37]. Fig. 5 shows the mechanism of ATN degradation by UV/PMS/MW process.

Fig. 4C explains the interaction between the initial concentration and UV irradiation time on the ATN degradation rate. At all initial concentrations, with the increase of irradiation time, initially the degradation efficiency was

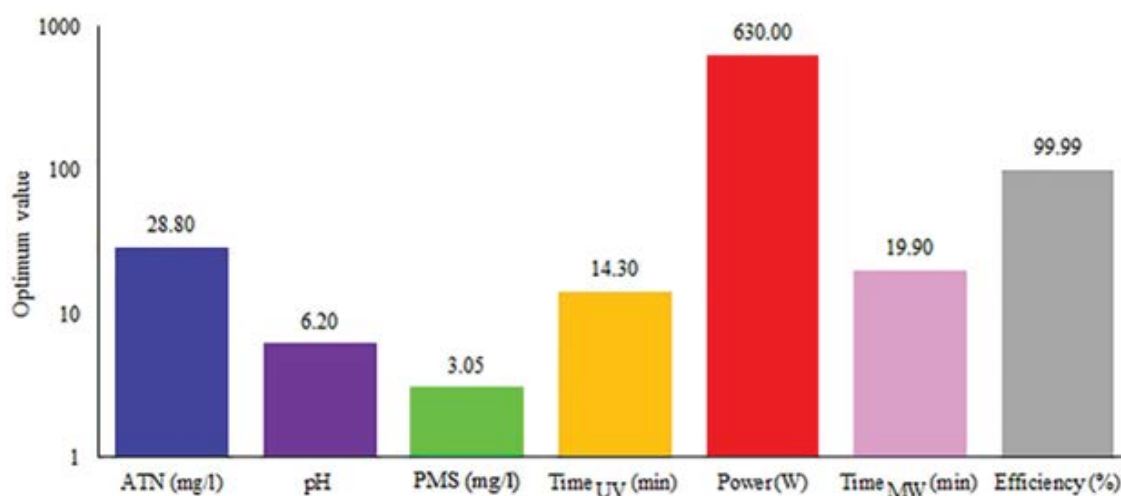


Fig. 3. Particle swarm optimization algorithm results, the optimal value of the input parameters and highest degradation efficiency. (ATN = 28.80 mg/L, pH = 6.20, PMS = 3.05 mg/L, UV time = 14.30 min, MW time = 19.90 min, and MW power = 630 W).

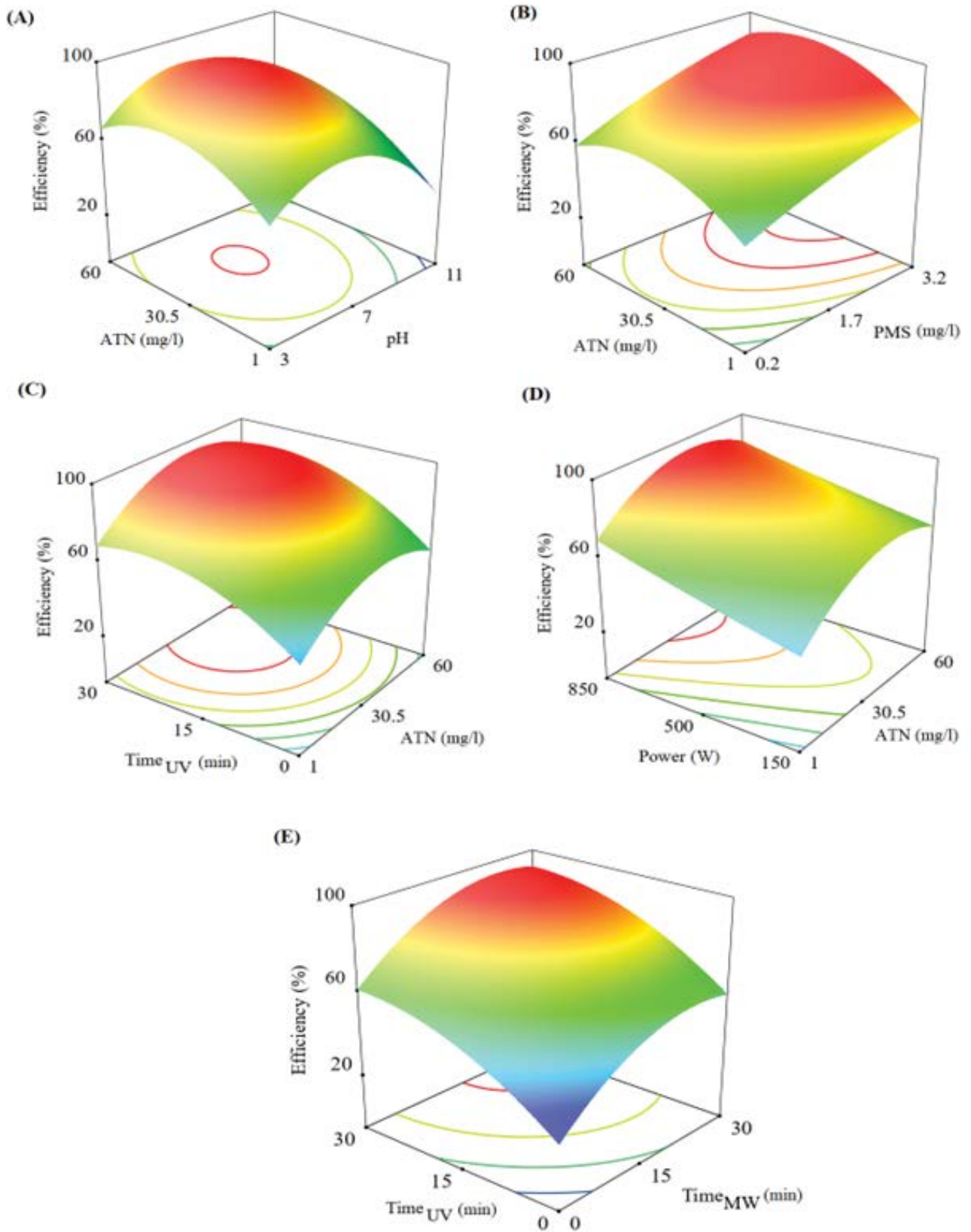


Fig. 4. 3-Dimensional graphs of artificial neural network prediction showing the interaction effects of input variables on the atenolol degradation rate.

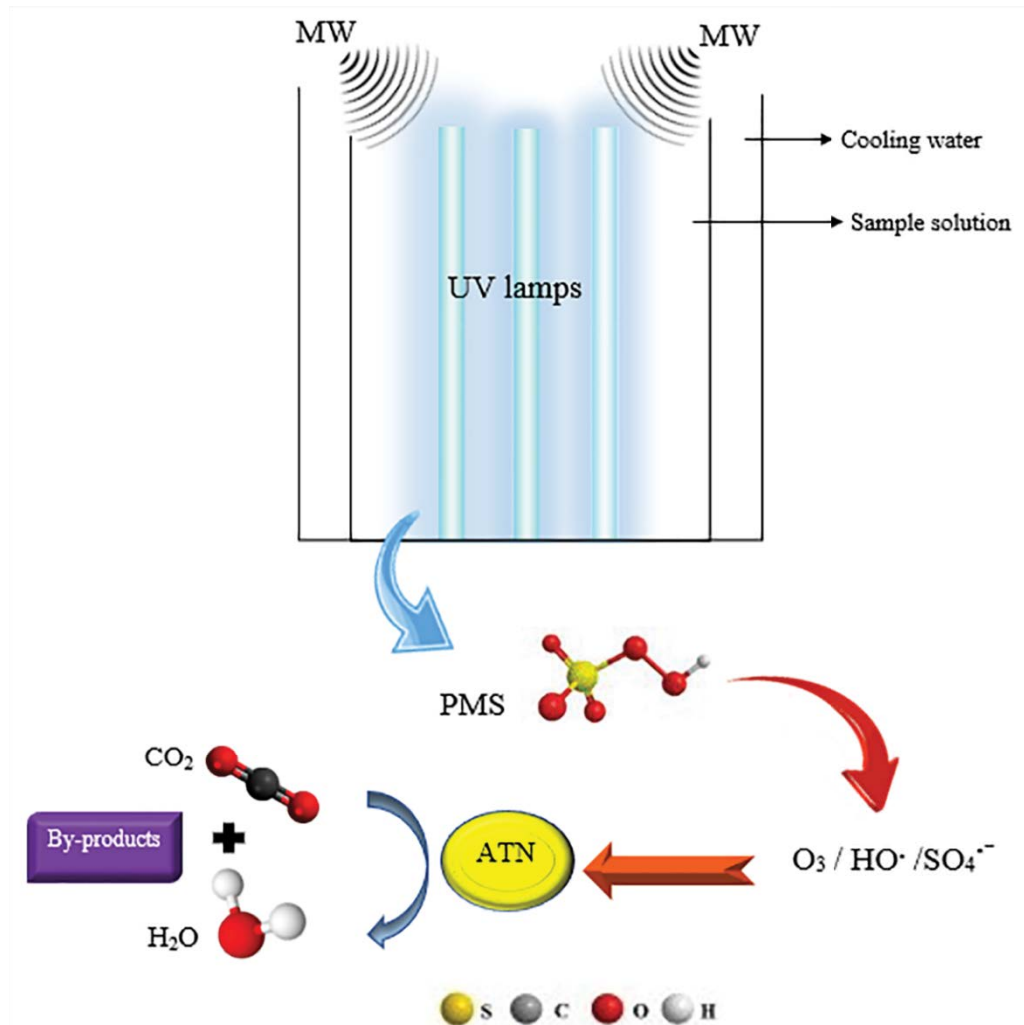


Fig. 5. Atenolol degradation mechanism by UV/PMS/MW process.

increased with a steep slope. However, after reaching the optimal time, which is about 15 min, the slope of the efficiency decreased with the increase of time, and after that the efficiency remained constant. Also, according to Shi et al. [43] research, on the degradation of 4 drugs, including atenolol, by UV/H₂O₂, the results showed that the components may absorb UV light and react with OH•, which would reduce the steady-state concentration of radicals in wastewater, so UV causes degradation. Also two different mechanisms might be involved in the activation of PMS by UV radiation. The first one is the rift of the O–O bond by energy input of UV, and the other PMS activation assumption is the production of the electron by the interaction of UV radiation with water molecule [44], as shown in Eqs. (1)–(3).



Fig. 4D shows the interaction between ATN initial concentration and MW power on the ATN degradation rate. It is understood that, the MW power is almost linearly related to the degradation efficiency, at all ATN initial concentrations. With the enhancement of this parameter, the degradation efficiency has increased. Ai et al. [45] worked on degradation of 4-chlorophenol by microwave irradiation. The study shows that 4-CP could not be degraded by MW alone but the efficiencies of other AOPs can be sharply increased in the presence of MW. Also, according to Liu et al. [46], the MW efficacy on the degradation of ofloxacin has been as follows; the reaction speed increases as the microwave power from 100 to 400 W. However, the degradation rate of ofloxacin was reduced to very high microwave power conditions (600 W) [46]. In conformity with Yang et al. [47], MW radiation generate sulfate free radicals by provide the needed activation energy for breaking down the chemical bonds. Then, generated SO₄^{•-} may react straightly with organic molecules also OH may be created due to the SO₄^{•-} and the created OH may also play a part in the degradation too, MW energy behave as an effectual activator of PMS to produce SO₄^{•-}, as shown in Eq. (4) [48].



The interaction between the UV time and MW time variables on the ATN degradation rate can be seen in Fig. 4E. The effect of MW time on degradation efficiency is similar to UV radiation time, which is non-linear. With increasing MW time, the degradation efficiency initially was increased with a steep slope, but after reaching the optimal time, which is about 20 min, the efficiency was decreased with increasing slope time, and after that the efficiency remained constant. Both parameters have had similar and identical effects on each other, so that ATN degradation rate has increased with increase of both variables. Table 3 shows the results for the present study in comparison with the previous studies.

3.4. Sensitivity analysis

Sensitivity analysis was performed by Pearson correlation method to determine which parameter has the greatest effect on degradation efficiency. Fig. 6 reveals that the order of effect of the input parameters on the degradation efficiency based on the correlation coefficient were as follows: pH, ATN, PMS, power, MW-time and UV-time.

3.5. Kinetics reaction

Kinetics study is necessary to evaluate the degradation rate and conduct of ATN as subordinate of reaction time. Table 4 presents the equation of pseudo-zero, first-order and second-order kinetic models used in this research. Kinetic diagrams and those proportion to the results of ATN degradation efficiency by UV/PMS/MW are shown in Fig. 7. As the degradation rate constants (k) and correlation coefficients (R²) are displayed in Table 5, second-order explained ATN degradation (R² > 0.9016) better in comparison of other kinetic models. The result was similar with Yu et al. [5] who worked on degradation of ATN via integrated UV/ozone/peroxymonosulfate process.

3.6. Effect of water matrix

Nitrate (NO₃⁻), chloride (Cl⁻) and HA as regular compound of natural dissolved organic matter (NDOM), are present in surface and underground waters. HA and nitrate can attract light in the UV range [40]. Fig. 8 shows the

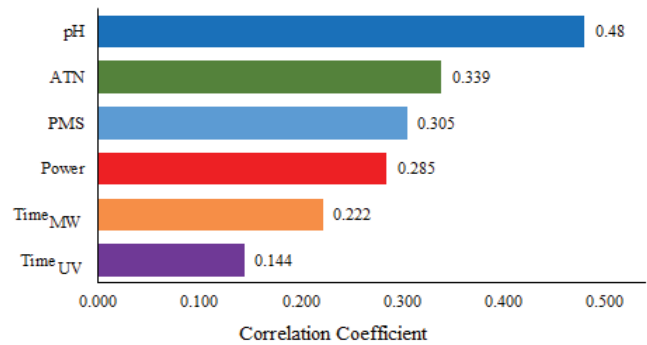


Fig. 6. Sensitivity analysis using Pearson correlation.

Table 4 Kinetic equations in the present study

Kinetic type	Equation	Integrated form	Eq. No.
Pseudo-zero-order	$rc = \frac{dc}{dt} = -k_0$	$C_e - C_0 = -k_0 t$	(5)
Pseudo-first-order	$rc = \frac{dc}{dt} = -k_1 C$	$\ln\left(\frac{C_e}{C_0}\right) = -k_1 t$	(6)
Pseudo-second-order	$rc = \frac{dc}{dt} = -k_2 C_2$	$\left(\frac{1}{C_e}\right) - \left(\frac{1}{C_0}\right) = k_2 t$	(7)

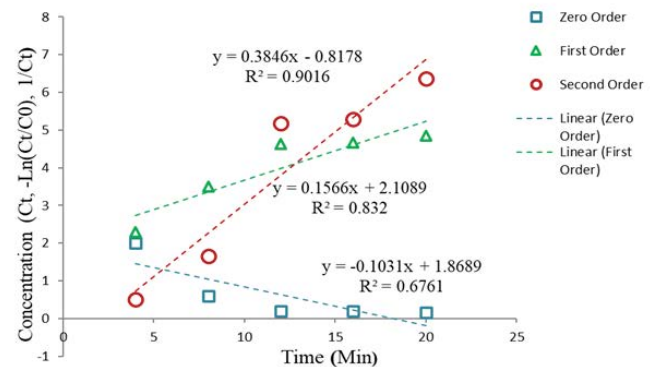


Fig. 7. Kinetic fitted plots of atenolol degradation: zero-order, first-order, and second-order, in optimal condition.

Table 3 Comparative evaluation of the results for this study with previous studies

Pollutant	Degradation method	pH	Initial concentration of pollutant	PMS concentration	UV time (min)	MW time (min)	MW power (W)	Efficiency (%)	References
Atenolol	UV/PMS	7	20 μM	80 μM	30	–	–	99.85	[49]
Atenolol	PMS/BiOCl@Fe ₃ O ₄	6.5	2.5 mg/L	0.1 mM	–	–	–	99.99	[37]
Atrazine	PMS/HA/WTRs	3	10 μM	0.5 mM	–	–	–	95	[50]
P-nitrophenol	PMS/MnFe ₂ O ₄ /MW	7	20 mg/L	2 mM	–	2	500	97	[51]
Atenolol	PMS/UV/MW	6.2	28.8 mg/L	3.05 mg/L	14.30	19.90	630	99.99	Present study

Table 5
Kinetic parameters of different models for atenolol degradation

Model	K	R ²
Pseudo-zero-order	-0.1031	0.6761
Pseudo-first-order	0.1566	0.832
Pseudo-second-order	0.3846	0.9016

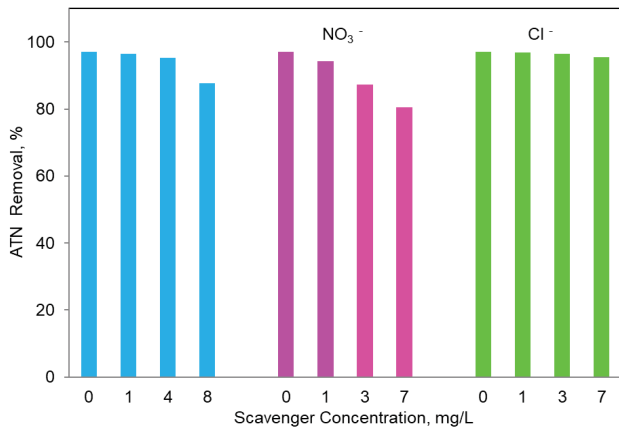
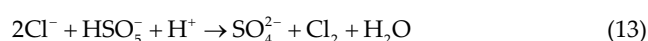
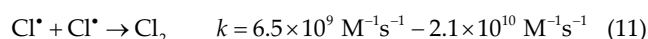
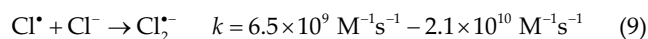
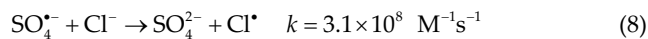


Fig. 8. Effect of scavengers on atenolol degradation, in optimal condition.

influence of these three confounders in various concentrations on the degradation of ATN. As clearly seen, the presence of 1–4 mg/L HA decreased the degradation rate of ATN from 97.3% to 95.26%. Also, further addition of HA up to 8 mg/L reduced ATN degradation to 87.76%. On the other hand, increasing NO₃⁻ to 7 mg/L has reduced the efficiency to 80.5%. As shown in Fig. 7, increasing chloride did not significantly alter the degradation of ATN, so that at the highest concentration decreased only about 2%. Nitrate and HA showed scavenging effect in high concentration for sulfate radical. They can absorb light in the UV range and act as a filter for the UV radiation [14]. Also, the chloride ion can scavenge free radicals produced in AOPs. Chloride has an inhibitory effect on the use of PMS and sulfate radicals in the process and leads to the formation of Cl[•] and Cl₂, which are less reactive oxidants [Eqs. (8)–(13)] [52–54].



4. Conclusion

The results of using hybrid UV/PMS/MW processes revealed that enhancing the PMS dosage or MW power increased ATN degradation efficiency. ATN can be degraded at neutral pH, which makes heat-activated PMS oxidation as a feasible choice to eliminate it from wastewater. The optimal value of the input parameters, which are ATN, pH, PMS, UV time, MW time and power, were equal to 28.80 mg/L, 6.20 mg/L, 3.05 mg/L, 14.30 min, 19.90 min and 630 W, which leads to the highest degradation efficiency of 99.99%. HA and NO₃⁻ limited ATN degradation, and the restrictive effect was increased with the increase of their concentrations, while the presence of Cl⁻ had not inhibitory effect on the degradation process. According to the obtained results from sensitivity analysis, pH was the most important parameter, and after that, the initial ATN concentration affect positively on ATN degradation efficiency. The kinetic investigation demonstrated that the adsorption process followed the second-order model. UV/PMS/MW proved to be an efficient method for ATN degradation as this method has high removal efficiency and it is relatively easy and fast. Perhaps the biggest disadvantage of the AOP process is its costs. The most significant are the operating and maintenance costs from the necessary energy and chemical reagents to operate the system.

In the future, UV/PMS/MW process, with very high efficiency on the finding of this study, will be an excellent advanced oxidation process for degradation of emerging pollutants such as atenolol, with low biodegradability in pre and post treatments units of municipal and industrial water and wastewater treatment plants.

Ethical code

The ethics code of this research is IR.MUI.RESEARCH.REC.1398.347.

Conflicts of interest

The authors declare that they have no conflicts of interest.

Acknowledgments

This research was supported by Student Research committee of Isfahan University of Medical Sciences (Grant No. 198117).

References

- [1] X. Sun, G. Pan, H. Qi, Z. Sun, Dip-coating prepared nickel-foam composite cathodes with hydrophobic layer for atenolol elimination in electro-Fenton system, *J. Electroanal. Chem.*, 856 (2020) 113725, doi: 10.1016/j.jelechem.2019.113725.
- [2] A. Giacobbo, E.V. Soares, A.M. Bernardes, M.J. Rosa, M.N. Pinho, Atenolol removal by nanofiltration: a case-specific mass transfer correlation, *Water Sci. Technol.*, 81 (2020) 210–216.
- [3] Y. Gao, N. Gao, J. Chen, J. Zhang, D. Yin, Oxidation of β -blocker atenolol by a combination of UV light and chlorine: kinetics, degradation pathways and toxicity assessment, *Sep. Purif. Technol.*, 231 (2020) 115927, doi: 10.1016/j.seppur.2019.115927.

- [4] K. Govindan, V.D.W. Sumanasekara, A. Jang, Mechanisms for degradation and transformation of β -blocker atenolol via electrocoagulation, electro-Fenton, and electro-Fenton-like processes, *Environ. Sci.: Water Res. Technol.*, 6 (2020) 1465–1481.
- [5] X. Yu, W. Qin, X. Yuan, L. Sun, F. Pan, D. Xia, Synergistic mechanism and degradation kinetics for atenolol elimination via integrated UV/ozone/peroxymonosulfate process, *J. Hazard. Mater.*, 407 (2021) 124393, doi: 10.1016/j.jhazmat.2020.124393.
- [6] Z. Huo, S. Wang, Q. Zou, H. Shao, G. Xu, Radiolysis of cardiovascular drug atenolol in aqueous solution by electron beam: effect of water components and persulfate addition, *Radiat. Phys. Chem.*, 184 (2021) 109458, doi: 10.1016/j.radphyschem.2021.109458.
- [7] A. Hassani, J. Scaria, F. Ghanbari, P.V. Nidheesh, Sulfate radicals-based advanced oxidation processes for the degradation of pharmaceuticals and personal care products: a review on relevant activation mechanisms, performance, and perspectives, *Environ. Res.*, 217 (2023) 114789, doi: 10.1016/j.envres.2022.114789.
- [8] M.M. Amin, N. Bagheri, F. Mohammadi, B. Dehdashti, Sensitivity analysis with the Monte Carlo method and prediction of atenolol removal using modified multiwalled carbon nanotubes based on the response surface method: isotherm and kinetics studies, *Int. J. Chem. Eng.*, 2022 (2022) 4613023, doi: 10.1155/2022/4613023.
- [9] M. Farid, A. Mirvet, Y. Nacera, Degradation of atenolol in a rectangular staircase photocatalytic reactor with immobilized ZnO, *Chem. Eng. Technol.*, 44 (2021) 140–147.
- [10] F. Madjene, M. Assassi, O. Benhabiles, N. Yeddou-Mezenner, Optimisation and kinetic modelling of atenolol degradation by ZnO under solar irradiation, *Int. J. Environ. Anal. Chem.*, (2021) 1–12, doi: 10.1080/03067319.2021.1959567.
- [11] J.A. Garrido-Cardenas, B. Esteban-García, A. Agüera, J.A. Sánchez-Pérez, F. Manzano-Agugliaro, Wastewater treatment by advanced oxidation process and their worldwide research trends, *Int. J. Environ. Res. Public Health*, 17 (2020) 170, doi: 10.3390/ijerph17010170.
- [12] C.V. Rekhate, J.K. Srivastava, Recent advances in ozone-based advanced oxidation processes for treatment of wastewater—a review, *Chem. Eng. J. Adv.*, 3 (2020) 100031, doi: 10.1016/j.cej.2020.100031.
- [13] V. Kumar, M.P. Shah, Chapter 1 – Advanced Oxidation Processes for Complex Wastewater Treatment, M.P. Shah, Ed., *Advanced Oxidation Processes for Effluent Treatment Plants*, Elsevier, India, 2021, pp. 1–31.
- [14] Y. Yang, Y. Cao, J. Jiang, X. Lu, J. Ma, S. Pang, J. Li, Y. Zhou, C. Guan, Comparative study on degradation of propranolol and formation of oxidation products by UV/H₂O₂ and UV/persulfate (PDS), *Water Res.*, 149 (2019) 543–552.
- [15] R. Bajagain, S-W. Jeong, Degradation of petroleum hydrocarbons in soil via advanced oxidation process using peroxymonosulfate activated by nanoscale zero-valent iron, *Chemosphere*, 270 (2021) 128627, doi: 10.1016/j.chemosphere.2020.128627.
- [16] Q. Wang, P. Rao, G. Li, L. Dong, X. Zhang, Y. Shao, N. Gao, W. Chu, B. Xu, N. An, J. Deng, Degradation of imidacloprid by UV-activated persulfate and peroxymonosulfate processes: kinetics, impact of key factors and degradation pathway, *Ecotoxicol. Environ. Saf.*, 187 (2020) 109779, doi: 10.1016/j.ecoenv.2019.109779.
- [17] X. Chen, J. Zhou, Y. Chen, Y. Zhou, L. Ding, H. Liang, X. Li, Degradation of tetracycline hydrochloride by coupling of photocatalysis and peroxymonosulfate oxidation processes using CuO-BiVO₄ heterogeneous catalyst, *Process Saf. Environ. Prot.*, 145 (2021) 364–377.
- [18] T. Cai, L. Bu, Y. Wu, S. Zhou, Z. Shi, Accelerated degradation of bisphenol A induced by the interaction of EGCG and Cu(II) in Cu(II)/EGCG/peroxymonosulfate process, *Chem. Eng. J.*, 395 (2020) 125134, doi: 10.1016/j.cej.2020.125134.
- [19] J. Mohamadiyan, G. Shams-Khoramabadi, S.A. Mussavi, B. Kamarehie, Y. Dadban Shahamat, H. Godini, Aniline degradation using advanced oxidation process by UV/peroxy disulfate from aqueous solution, *Int. J. Eng. (IJE)*, 30 (2017) 684–690.
- [20] K. Song, F. Taghipour, M. Mohseni, Microorganisms inactivation by wavelength combinations of ultraviolet light-emitting diodes (UV-LEDs), *Sci. Total Environ.*, 665 (2019) 1103–1110.
- [21] E. Ryan, S. Turkmen, S. Benson, An investigation into the application and practical use of (UV) ultraviolet light technology for marine antifouling, *Ocean Eng.*, 216 (2020) 107690, doi: 10.1016/j.oceaneng.2020.107690.
- [22] Y.D. Shahamat, M. Masihpour, P. Borghei, S.H. Rahmati, Removal of azo red-60 dye by advanced oxidation process O₃/UV from textile wastewaters using Box–Behnken design, *Inorg. Chem. Commun.*, 143 (2022) 109785, doi: 10.1016/j.inoche.2022.109785.
- [23] G. Ozyildiz, T. Olmez-Hanci, I. Arslan-Alaton, Effect of nano-scale, reduced graphene oxide on the degradation of bisphenol A in real tertiary treated wastewater with the persulfate/UV-C process, *Appl. Catal., B*, 254 (2019) 135–144.
- [24] P.P. Falciglia, E. Gagliano, V. Brancato, G. Malandrino, G. Finocchiaro, A. Catalfo, G.D. Guidi, S. Romano, P. Roccaro, F.G.A. Vagliasindi, Microwave based regenerating permeable reactive barriers (MW-PRBs): proof of concept and application for Cs removal, *Chemosphere*, 251 (2020) 126582, doi: 10.1016/j.chemosphere.2020.126582.
- [25] L. Hu, P. Wang, T. Shen, Q. Wang, X. Wang, P. Xu, Q. Zheng, G. Zhang, The application of microwaves in sulfate radical-based advanced oxidation processes for environmental remediation: a review, *Sci. Total Environ.*, 722 (2020) 137831, doi: 10.1016/j.scitotenv.2020.137831.
- [26] W. Wang, Z. Li, M. Zhang, C. Sun, Preparation of 3D network CNTs-modified nickel foam with enhanced microwave absorptivity and application potential in wastewater treatment, *Sci. Total Environ.*, 702 (2020) 135006, doi: 10.1016/j.scitotenv.2019.135006.
- [27] F. Wang, C. Wu, Q. Li, Treatment of refractory organics in strongly alkaline dinitrodiazophenol wastewater with microwave irradiation-activated persulfate, *Chemosphere*, 254 (2020) 126773, doi: 10.1016/j.chemosphere.2020.126773.
- [28] J.V. Tu, Advantages and disadvantages of using artificial neural networks versus logistic regression for predicting medical outcomes, *Clin. Epidemiol.*, 49 (1996) 1225–1231.
- [29] S. Panda, N.P. Padhy, Comparison of particle swarm optimization and genetic algorithm for FACTS-based controller design, *Appl. Soft Comput.*, 8 (2008) 1418–1427.
- [30] M. Berkani, B.K. Bouchareb, M. Bouhelassa, Y. Kadmi, Photocatalytic degradation of industrial dye in semi-pilot scale prototype solar photoreactor: optimization and modeling using ANN and RSM based on Box–Wilson approach, *Top. Catal.*, 63 (2020) 964–975.
- [31] J. Jawad, A.H. Hawari, S.J. Zaidi, Artificial neural network modeling of wastewater treatment and desalination using membrane processes: a review, *Chem. Eng. J.*, 419 (2021) 129540, doi: 10.1016/j.cej.2021.129540.
- [32] M. Piponski, K. Peleshok, L. Logoyda, L. Kravchuk, V. Piatnochka, U. Zakharchuk, Efficient validated HPLC/UV method for determination of valsartan and atenolol in dosage form and *in vitro* dissolution studies, *Biointerface Res. Appl. Chem.*, 10 (2020) 6669–6675.
- [33] F. Mohammadi, B. Bina, H. Karimi, S. Rahimi, Z. Yavari, Modeling and sensitivity analysis of the alkylphenols removal via moving bed biofilm reactor using artificial neural networks: comparison of Levenberg Marquardt and particle swarm optimization training algorithms, *Biochem. Eng. J.*, 161 (2020) 107685, doi: 10.1016/j.bej.2020.107685.
- [34] N. Lotfi, J. Tamouk, M. Farmanbar, 3-SAT problem a new memetic-PSO algorithm, *arXiv*, (2013) 13065070, doi: 10.48550/arXiv.1306.5070.
- [35] A.K. Rathankumar, V.K. Vaithyanathan, K. Saikia, S.S. Anand, V.K. Vaidyanathan, H. Cabana, Effect of alkaline treatment on the removal of contaminants of emerging concern from municipal biosolids: modelling and optimization of process parameters using RSM and ANN coupled GA, *Chemosphere*, 286 (2022) 131847, doi: 10.1016/j.chemosphere.2021.131847.
- [36] V. Bhatia, A. Dahir, A.K. Ray, Photocatalytic degradation of atenolol with graphene oxide/zinc oxide composite:

- optimization of process parameters using statistical method, *J. Photochem. Photobiol., A*, 409 (2021) 113136, doi: 10.1016/j.jphotochem.2021.113136.
- [37] Y. Wu, Z. Fang, Y. Shi, H. Chen, Y. Liu, Y. Wang, W. Dong, Activation of peroxymonosulfate by BiOCl/Fe₃O₄ catalyst for the degradation of atenolol: kinetics, parameters, products and mechanism, *Chemosphere*, 216 (2019) 248–257.
- [38] E. Hapeshi, A. Achilleos, M.I. Vasquez, C. Michael, N.P. Xekoukoulotakis, D. Mantzavinos, D. Kassinos, Drugs degrading photocatalytically: kinetics and mechanisms of ofloxacin and atenolol removal on titania suspensions, *Water Res.*, 44 (2010) 1737–1746.
- [39] Y. Xu, Z. Lin, Y. Wang, H. Zhang, The UV/peroxymonosulfate process for the mineralization of artificial sweetener sucralose, *Chem. Eng. J.*, 317 (2017) 561–569.
- [40] X. Liu, L. Fang, Y. Zhou, T. Zhang, Y. Shao, Comparison of UV/PDS and UV/H₂O₂ processes for the degradation of atenolol in water, *J. Environ. Sci.*, 25 (2013) 1519–1528.
- [41] P.V. Gayathri, S. Yesodharan, E.P. Yesodharan, Microwave/persulfate assisted ZnO mediated photocatalysis (MW/PS/UV/ZnO) as an efficient advanced oxidation process for the removal of RhB dye pollutant from water, *J. Environ. Chem. Eng.*, 7 (2019) 103122, doi: 10.1016/j.jece.2019.103122.
- [42] D. Miao, J. Peng, X. Zhou, L. Qian, M. Wang, L. Zhai, S. Gao, Oxidative degradation of atenolol by heat-activated persulfate: kinetics, degradation pathways and distribution of transformation intermediates, *Chemosphere*, 207 (2018) 174–182.
- [43] Y. Shi, G. Shen, J. Geng, Y. Fu, S. Li, G. Wu, L. Wang, K. Xu, H. Ren, Predictive models for the degradation of 4 pharmaceutically active compounds in municipal wastewater effluents by the UV/H₂O₂ process, *Chemosphere*, 263 (2021) 127944, doi: 10.1016/j.chemosphere.2020.127944.
- [44] J. Rodríguez-Chueca, C. García-Cañibano, M. Sarro, Á. Encinas, C. Medana, D. Fabbri, P. Calza, J. Marugán, Evaluation of transformation products from chemical oxidation of micropollutants in wastewater by photo-assisted generation of sulfate radicals, *Chemosphere*, 226 (2019) 509–519.
- [45] A. Zhihui, Y. Peng, L. Xiaohua, Degradation of 4-chlorophenol by microwave irradiation enhanced advanced oxidation processes, *Chemosphere*, 60 (2005) 824–827.
- [46] X. Liu, F. Huang, Y. Yu, P. Zhao, Y. Zhou, Y. He, Y. Xu, Y. Zhang, Ofloxacin degradation over Cu–Ce tyre carbon catalysts by the microwave assisted persulfate process, *Appl. Catal., B*, 253 (2019) 149–159.
- [47] S. Yang, P. Wang, X. Yang, G. Wei, W. Zhang, L. Shan, A novel advanced oxidation process to degrade organic pollutants in wastewater: microwave-activated persulfate oxidation, *J. Environ. Sci.*, 21 (2009) 1175–1180.
- [48] H. Xia, C. Li, G. Yang, Z. Shi, C. Jin, W. He, J. Xu, G. Li, A review of microwave-assisted advanced oxidation processes for wastewater treatment, *Chemosphere*, 287 (2022) 131981, doi: 10.1016/j.chemosphere.2021.131981.
- [49] X. Liu, T. Zhang, Y. Zhou, L. Fang, Y. Shao, Degradation of atenolol by UV/peroxymonosulfate: kinetics, effect of operational parameters and mechanism, *Chemosphere*, 93 (2013) 2717–2724.
- [50] H. Zhang, X. Liu, C. Lin, X. Li, Z. Zhou, G. Fan, J. Ma, Peroxymonosulfate activation by hydroxylamine-drinking water treatment residuals for the degradation of atrazine, *Chemosphere*, 224 (2019) 689–697.
- [51] Y. Pang, H. Lei, Degradation of p-nitrophenol through microwave-assisted heterogeneous activation of peroxymonosulfate by manganese ferrite, *Chem. Eng. J.*, 287 (2016) 585–592.
- [52] F. Ghanbari, M. Moradi, Application of peroxymonosulfate and its activation methods for degradation of environmental organic pollutants: review, *Chem. Eng. J.*, 310 (2017) 41–62.
- [53] A. Hassani, P. Eghbali, F. Mahdipour, S. Wacławek, K.A. Lin, F. Ghanbari, Insights into the synergistic role of photocatalytic activation of peroxymonosulfate by UVA-LED irradiation over CoFe₂O₄-rGO nanocomposite towards effective Bisphenol A degradation: performance, mineralization, and activation mechanism, *Chem. Eng. J.*, 453 (2023) 139556, doi: 10.1016/j.cej.2022.139556.
- [54] S. Madihi-Bidgoli, S. Asadnezhad, A. Yaghoot-Nezhad, A. Hassani, Azurobine degradation using Fe₂O₃@multi-walled carbon nanotube activated peroxymonosulfate (PMS) under UVA-LED irradiation: performance, mechanism and environmental application, *J. Environ. Chem. Eng.*, 9 (2021) 106660, doi: 10.1016/j.jece.2021.106660.